Electronic Supplementary Material (ESI) for Physical Chemistry Chemical Physics.

Supporting Information

Loading of ionic compounds into metal-organic frameworks: A joint theoretical and experimental study for the case of La^{3+}

Wei Guo, Jinxuan Liu, Peter G. Weidler, Jianxi Liu, Tobias Neumann, Denis Danilov, Wolfgang Wenzel, Claus Feldmann and Christof Wöll

Inductively Coupled Plasma Optical Emission Spectrometer (ICP-OES,Perkin Elmer, USA) measurement were carried out using a Perkin-Elmer model Optima 8300 DV equipped with a GemTipTM Crossflow Nebuliser (Perkin Elmer, USA). X-ray photoelectron spectroscopy (XPS) measurement were performed on a Kalpha spectrometer (ThermoFisher Scientific, East Grinstead, U.K.) using a microfocused, monochromated Al Kα X-ray source (400 μm spot size). Infra red reflection absorption spectroscopy (IRRAS) data were recorded using a Biorad Excalibur FTIR spectrometer (FTS 3000) equipped with a grazing incidence reflection unit (Biorad Uniflex) and a narrow band MCT detector. X-ray diffraction (XRD) measurements for out-of-plane (co-planar orientation) were carried out using Bruker D8-Advance diffractometer equipped with a position sensitive detector (PSD) Lynxeye® in θ-θ geometry, variable divergence slit and 2.3° Soller-slit was used on the secondary side. XRD measurements for in-plane (non-coplanar orientation) were carried out using Bruker D8 Discover equipped with a quarter Eulerian cradle, tilt-stage and 2.3° Soller-slits were installed in both sides. A Göbel-mirror, and a PSD Lynxeye® in θ-2θ geometry, were applied in the measurement. The Cu-anodes which utilize the Cu Kα1, 2-radiation (λ= 0.154018 nm) was used in both instrument. The measurement was carried out in the range of 2θ = 5°- 20° at a scan step of 0.02° at 40 kV and 30 mA. ImageJ software with a Dropsnake plugin was used to measure the water contact angle.

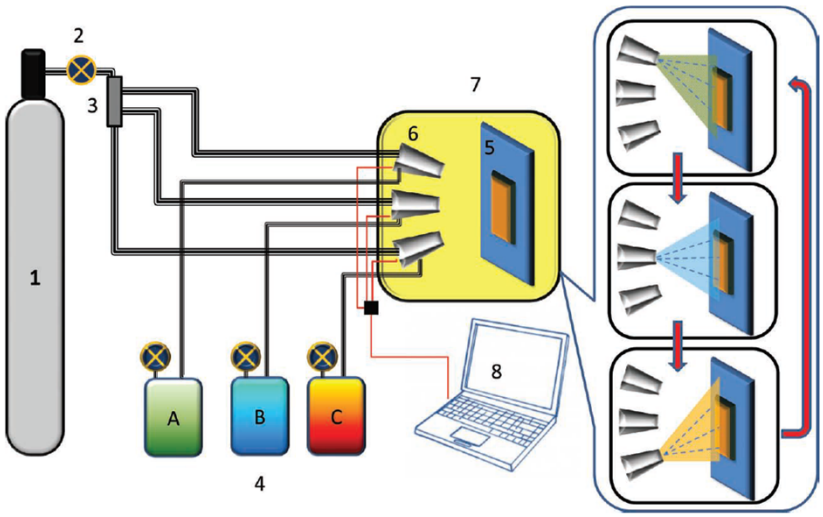

Fig. S1 Setup employed for the fabrication of MOF thin films with the spray method: (1) Gas supply, (2) gas fl ow controller (3) three-way valve gas distributor (4) (A, B, C) solutions storage containers (5) sample holder (6) dosing valves, (7) spray chamber, (8) PC. (H. K. Arslan, O. Shekhah, J. Wohlgemuth, M. Franzreb, R. A. Fischer and C. Woll, Advanced functional materials, 2011, 21, 4228-4231.).

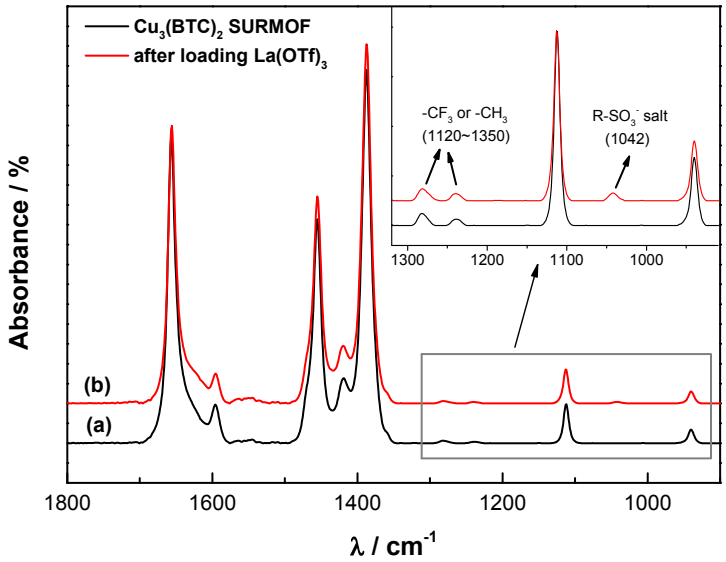

Fig. S2 IR spectroscopy of (a) 20 cycles of $Cu_3(BTC)_2$ MOF thin films and (b) after loading $La(OTf)_3$.

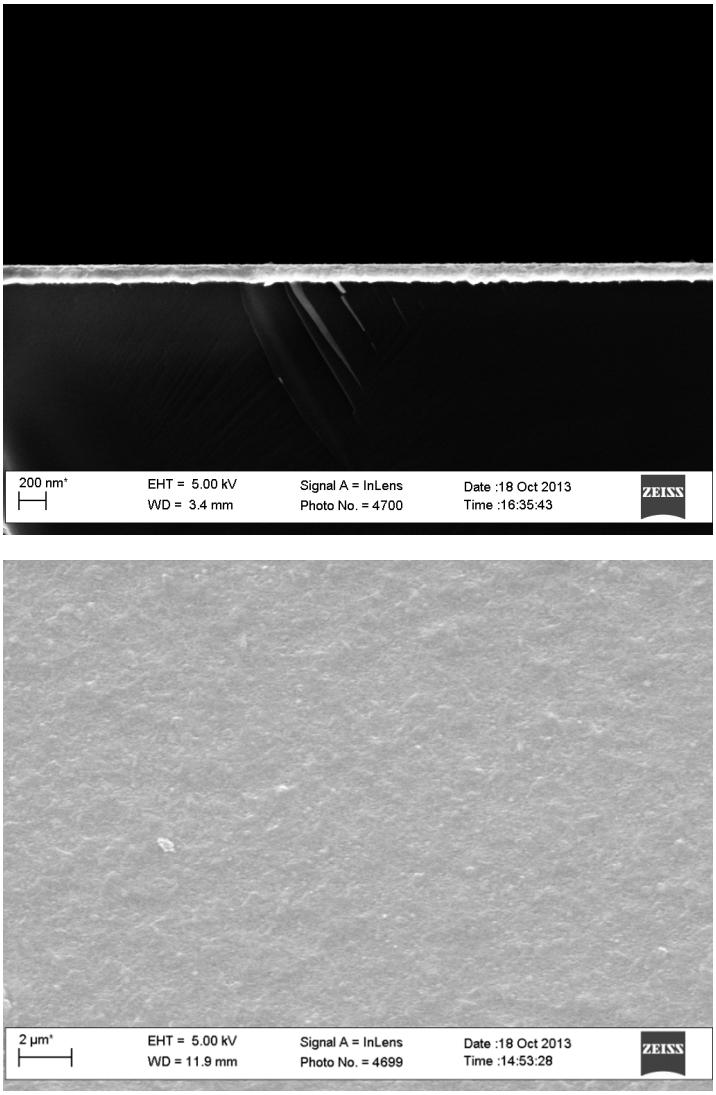

Fig. S3 Scanning Electron Microscope (SEM) of 20 cycles of $Cu_3(BTC)_2$ MOF thin films

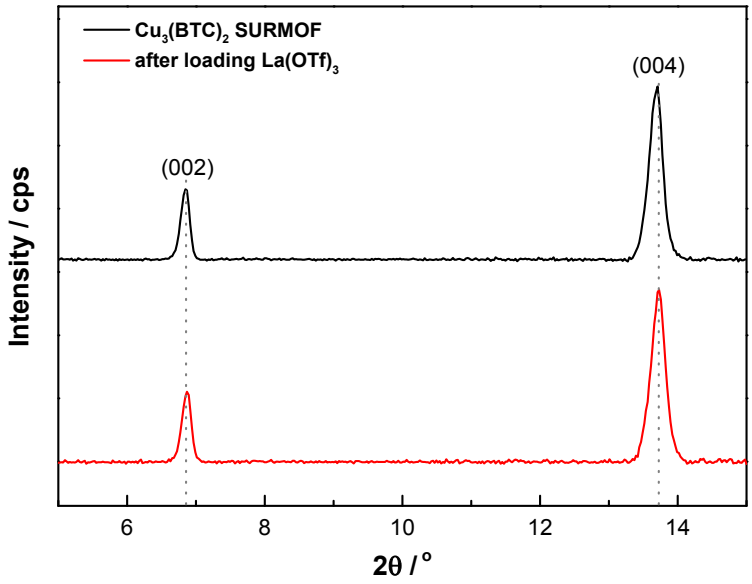

Fig. S4 X-ray diffraction patterns of $La(OTf)_3@Cu_3(BTC)_2$ SURMOF (black) and after ultrasonic cleaning in dichloromethane for 15min

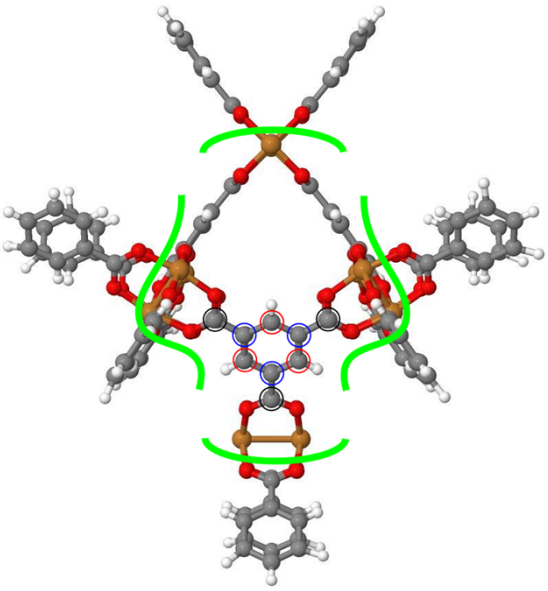

Fig. S5 Calculation of partial charges of the $Cu_3(BTC)_2$ MOF.

To achieve convergence in the DFT calculation only a small fraction of the P1 MOF unit cell including all atom types was taken into account. Dangling bonds were avoided by adding hydrogen atoms. The values for the charges were averaged over all atoms of each atom type. To avoid edge effects only the atoms within the green boundaries were taken into account. Atom types are Cu, O, H, C (black circles), aromatic C1 (blue circles) and aromatic C2 (red circles).

Partial charges were calculated using the ESP fit implemented in the DFT code TURBOMOLE1 using SV(P) basis and b3-lyp functional with damping and Fermi. While this was straight forward for the OTf- ions, the (cubic, not primitive) unit cell of the MOF was too large to achieve convergence. We performed DFT calculations for a subsection of the unitcell as illustrated in Fig S5. Dangling bonds were avoided by adding hydrogen atoms. Final partial charges were then calculated by averaging the single atom partial charges over all atoms of each type. The resulting partial charges are displayed in table S1

Atom type	Partial charge
Cu	1.012914 (1.3e-6)
O	-0.631583 (1.1e-6)
H	0.145153 (5e-7)
C	0.774928 (5e-6)
Aromatic C1	-0.067864 (4e-6)
Aromatic C2	-0.101650 (3e-6)

Table S1 Values and standard deviation (in brackets) for the partial charges of the atom types in the MOF.

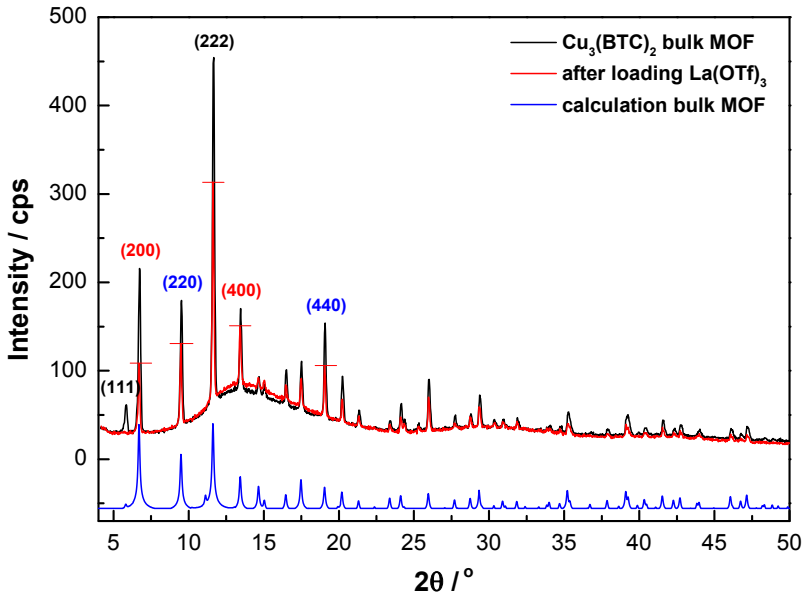

Fig. S6 X-ray diffraction patterns of bulk $Cu_3(BTC)_2$ MOF (black), after loading La(OTf)3 (red) and calculated data(blue).

Name	Amount %	Cu/La ratio
La^{3+}	0.80	
Cu^{2+}	4.30	5.37

Table S2 Element composition determined by X-ray photoelectron spectrum (XPS) analysis for $La(OTf)_3@Cu_3(BTC)_2$ MOF thin films.

Name	Wavelength nm	Amount mg/L	Cu/La ratio
La^{3+}	224.700	3.28	
	327.393	3.32	
Cu^{2+}	379.478	0.45	
	384.902	0.45	7.3

Table S3 Element composition determined by Inductively Coupled Plasma Optical Emission Spectrometry (ICP-OES) analysis for $La(OTf)_3@Cu_3(BTC)_2$ MOF thin films.

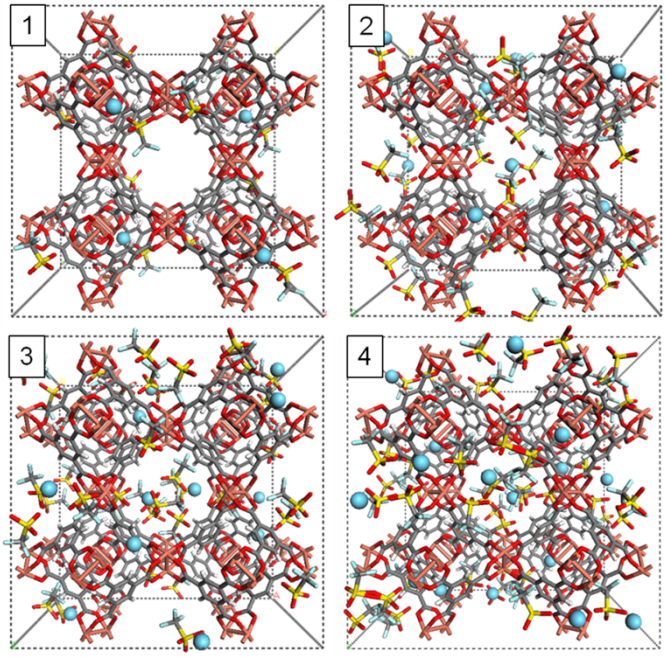

Fig. S7 Schematic structure of single $La(OTf)_3$ (1), 2 $La(OTf)_3$ in (2), 3 $La(OTf)_3$ (3) and in 4 $La(OTf)_3$ $Cu_3(BTC)_2$ MOF.

1 R. Ahlrichs, M. Bar, M. Haser, H. Horn and C. Kolmel, Chemical Physics Letters, 1989, 162, 165-169.